Three-Dimensional Microstructured Lattices for Oil Sensing

Aydin Sabouri,[1] Ali K. Yetisen,[2] Rashad Sadigzade,[1] Hany Hassanin,[3] Khamis Essa,[1,*] Haider Butt[1,*]

[1]School of Engineering, University of Birmingham, Birmingham B15 2TT, UK

[2] Harvard-MIT Division of Health Sciences and Technology, Massachusetts Institute of Technology, Cambridge, MA 02139, USA

[3] School of Mechanical and Aerospace Engineering, Kingston University, London, SW15 3DW, UK

Abstract

Monitoring of environmental contamination including oil pollution is important to protect marine ecosystems. A wide range of sensors are utilized in petroleum industry to measure various parameters such as viscosity, pressure, and flow. Here, we create an optical lattice mesh structure that can be used as an oil sensor integrated with optical fiber probing. The principle of operation of the sensor was based on light scattering, where the tested medium acted as a diffuser. Three different mesh-sized structures were analyzed by optical imaging, light transmission and scattering in the presence of supercut, diesel and stroke oil types within the meshes. The meshes were utilized as a medium for different types of oils and the optical diffusion and transmission were studied in the visible spectrum. Angle-resolved measurements were carried out to characterize light scattering behavior from the mesh structures. Different types of oils were identified based on the optical behavior of the lattice structure. The fabricated mesh structures can be utilized as a low-cost measurement device in oil sensing.

Keywords: lattice structures, oil detection, optical scattering, spectroscopy

Introduction

91 million barrels of oil is consumed daily for generating energy, driving machinery, and for the transportation industry.[1] Its fractions are used for manufacturing chemical products such as plastics, detergents, paints, and also have a wide range of applications in the healthcare industry. As a result of global industrialization and increasing mobility, the demand for petroleum products continues to rise.[2] This raises the need to improve the technical ability to efficiently extract oil, extend the production lines of existing oil fields, and discover new sources. One of the undesirable issues in the petroleum industry is oil leakage, which can result in economic losses and environmental pollution in soil and groundwater.[3] Therefore, development of an oil sensor for rapidly detecting oil is highly desirable.

Various portable sensors have been developed for the detection of oils.[4-6] Some of these instruments are miniature versions of the laboratory instruments. Typically detection of the oils was performed by analyzing their physical, electrical, optical, and chemical properties.[5] Viscosity is one of the main physical properties that have been investigated as it indicates the resultant degradation under oxidation, contamination, or stress.[4] Sensors that analyze viscosity are generally classified based on displacement and vibration.[5] For measuring kinematic viscosity, solid micro-displacement was adapted in capillary, rotational, and dropping ball viscometers. The main disadvantages of these sensors include complex structure, experimental calibration requirement, and low reliability.[7] The principle of micro-vibrational measurements is based on determining the dynamic output of the resonators in contact with the oil sample. However, the precision of these mechanisms highly depends on the temperature of the medium. Moreover, electrochemical oil sensors operate based on the measurement of voltage or current between the electrodes by using oil as a dielectric material. With this approach, real-time monitoring of oil can be achieved. However,

due to the conductivity variation of oil types depending on their temperature and brand, capacitive sensors based on oil permittivity have been developed.[5] Additionally, fluorescence spectroscopy has been used as an effective approach for monitoring oils in seawater. The molecules of an oil sample were excited to higher level by using a narrow-band light source and readouts were recorded. This method was limited to the ability of the oil sample to fluoresce or capability of adding fluorescence tracers to it.[6] The use of fiber optic sensing in the oil and gas industry has greatly expanded over the past two decades. Fiber optic sensors have been designed based on measuring liquid refractive index.[8] The changes in light energy were studied by bending and tapering optical fiber's cladding. Depending on the physical and optical properties of the core, the refractive index of medium can be accurately measured to the third decimal place. The other type of fiber optic sensors are hollow waveguides which have been used for detecting gases such as CO, CO_2, NH_3, H_2S, C_2H_2 and CH_4.[9]

In the present work, we investigated the optical characteristics of a lattice structure, which was used as a medium for detecting oil. This property was influenced by both physical and optical properties of the oil. The optical diffusion and transmission properties of the lattice structure were analyzed for different types of oils in the visible spectrum.

Fabrication of lattice structures

We developed an oil sensor consisting of titanium alloy (Ti-6Al-4V) lattices, which are a unique classification of cellular structures. This type of shape can be regarded as a space truss structure composed of struts, nodes with certain repeated arrangement in three-dimensional (3D) space. Among different cellular structures, lattices are the most attractive type due to their inherent advantages. Firstly, as compared to those disordered cellular foam, only a small portion of a lattice structure is needed to determine its properties for high degree of

orders.[10] Also one of their most definitive benefits is the capability of maintaining mechanical performance while the weight is reduced resulting in lower material costs and increasing design flexibility.[11] These structures can provide high energy absorption characteristics and thermal and acoustic insulation properties.[12] Metal mesh structures have been reported as band-pass filters in terahertz (THz) region.[13] Crack-template metal mesh (CT-MM) structures have been engineered to be used as transparent electromagnetic interference (EMI) shielding (~26 dB).[14] Also highly homogeneous light transmission and strong microwave shielding was observed. Additionally, metal mesh devices were used to localize the electromagnetic field for the detection of a biotin-streptavidin combination.[15] Lattice structures can also be designed to be stretchable for load bearing with high stiffness as well as bendable for compliant mechanism with large deformation.[16] Thus, lattice structures have potential in a wide range of applications such as biomedical implants, shock or vibration damping, and acoustic absorption.[17] In the present work, the optical characteristics of the meshes were utilized for oil detection.

The alloy cellular solids with high strength, low modulus and desirable deformation behavior have been manufactured through the cell shape design using selective laser melting (SLM) in additive manufacturing (AM). In AM, information of each layer is taken from a stereolithography (STL) format that is the pattern file sliced in approximated triangles and manufactured by a 3D printer.[18] In SLM, 3D printing of metal enables the fabrication of complex-shaped parts with fine geometries. Interaction of a propagated laser beam with powder surface melts and fuses selected powder layers on top of each other under an inert atmosphere to create a predesigned model. A Concept Laser M2 Cusing SLM system equipped with an Nd:YAG laser with a wavelength of 1075 nm, a constant beam spot size of 50 μm, a laser power of 200 W has been used to carry out to build the lattice samples under Argon. Figure 1a shows a schematic of the fabrication process. Thin layers of metal powder

are spread evenly using a recoating blade onto a building plate that is fixed to a movable building platform that moves vertically. Once the layer is spread, each slice is selectively scanned by the laser beam and fused to the previous scanned layers. This process is repeated until the part is completely built.

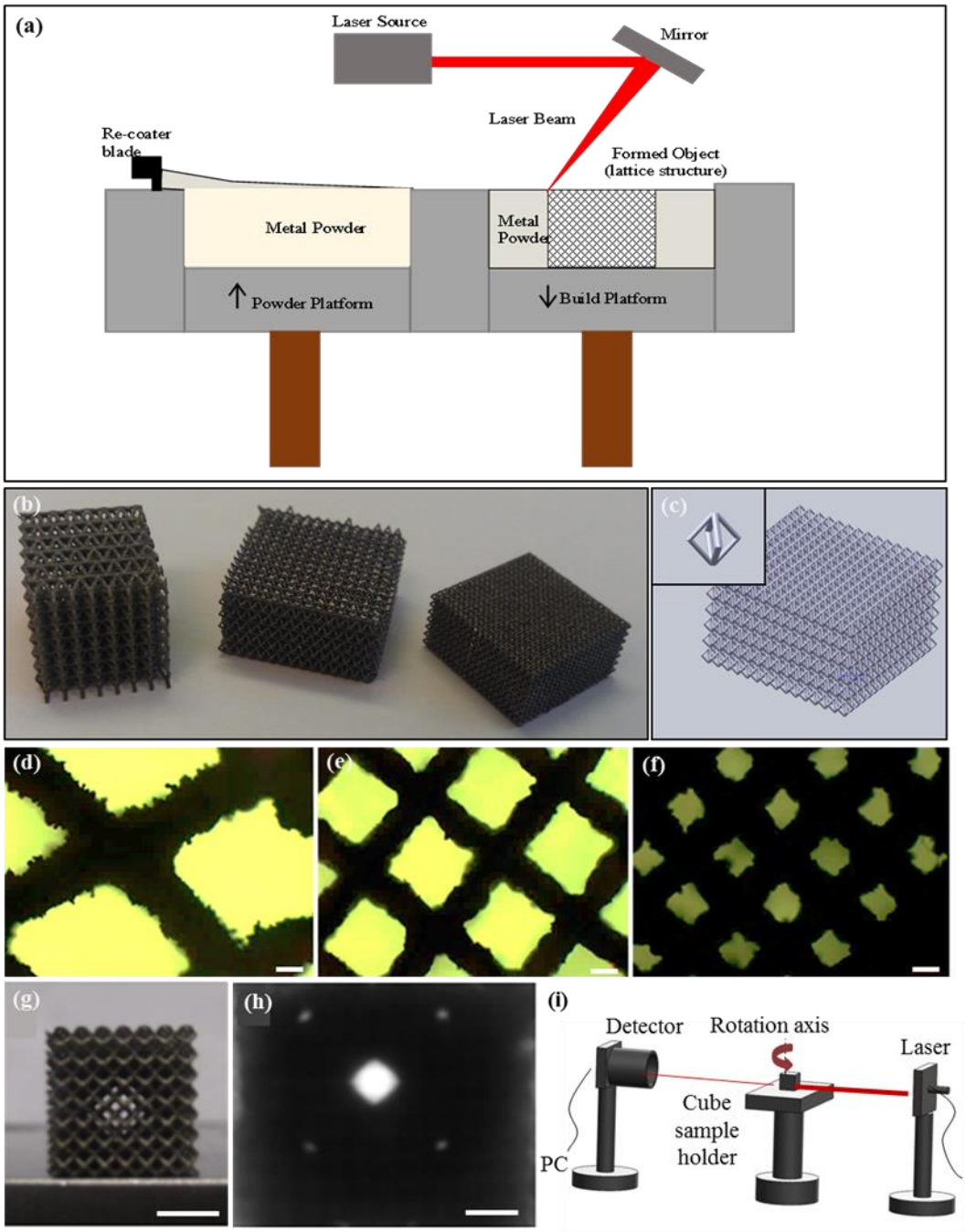

Figure 1. Fabrication of the 3D mesh structures. (a) Schematic of the selective laser melting process. (b) 3D-printed Ti-6Al-4V lattice for oil sensing mesh structures with the size of 1000, 700 and 400 μm (scale bar=1cm). (c) Schematic view of the mesh structures. Optical

microscope images of the microstructures having mesh sizes of (d) 1000, (e) 700 and (f) 400 μm (scale bars=200 μm). (g) 1000 μm mesh transmission window (scale bar=5 mm) (h) A magnified image of 1000 μm mesh (scale bar=2 mm). (i) Schematic diagram of the experimental setup used for measuring optical scattering from the meshes.

The lattice structures that were fabricated in the present work consisted of nodally-connected diamond unit cells with different mesh lengths of 400, 700 and 1000 μm (Figure 1b). Figure 1c shows a three-dimensional (3D) model of the lattice structure. Figure 1d-f show images of three different meshes under bright field illumination. The transmission window of the mesh structures is shown in Figure 1gand 1h. Optical transmission and scattering through the windows change in response to the medium within the meshes (air, water, oil etc). The optical scattering was measured experimentally using the setup shown in Figure 1i. The mesh material has a long life cycle and capable of operating in harsh environments. It has a compressive strength of 970 MPa and an elastic modulus of 113.8 GPa and melting point of 1604-1660 °C.[19]

Results and Discussions

Optical imaging of mesh structures with and without presence of oil was performed to study optical characteristics of the lattices. The optical transmission properties of mesh-sized structure of 700 μm with three different types of oils were tested. The parameters of studied oils at 25 ℃ are shown in Table 1.

Table 1. The properties of the oils studied in the present work

Oil Type	**Viscosity ($mm^2 s^{-1}$)**	**Density ($kg m^{-3}$)**
West Texas crude oil	4.9	870
Diesel	2.98	820
Stroke oil	45	870

For the other mesh sizes, optical imaging and transmission were measured in the presence of water and oil. The wetting property of Ti-6Al-4V has been shown to be modified by laser irradiation.[20] The processed samples were initially hydrophilic; however, over time, they become hydrophobic having contact angles of up to 137°. This change is determined by the surface chemistry due to increasing carbon content in Ti-6Al-4V. This hydrophobic behavior of the mesh structures enables removal of water by gravitational force over time (~1 min) and formation of oil droplets inside the mesh structures. Figure 2 demonstrates the difference between these meshes when water and oil are presented in transmission mode using a halogen white light source (Carl Zeiss HAL100). Figure 2(a-c) corresponds to a 400 μm periodic mesh lattice. The presence of the liquid altered the internal reflections of the incident light, resulting in different transmitted light within the same mesh structure. The periodic mesh structures have optical windows through which light travels unperturbed, when air is the medium. In the liquid, optical scattering takes place within the windows,[21, 22] the droplets of oil/water act as microlenses changing the path of light (Figure 2c).[23] Figure 2(d-f) shows an analogous effect for a mesh size of 1000 μm. After presenting the oil to the matrix, the transmitted light reduced 9% and 4% for both 700 μm and 1000 μm mesh sizes, respectively.

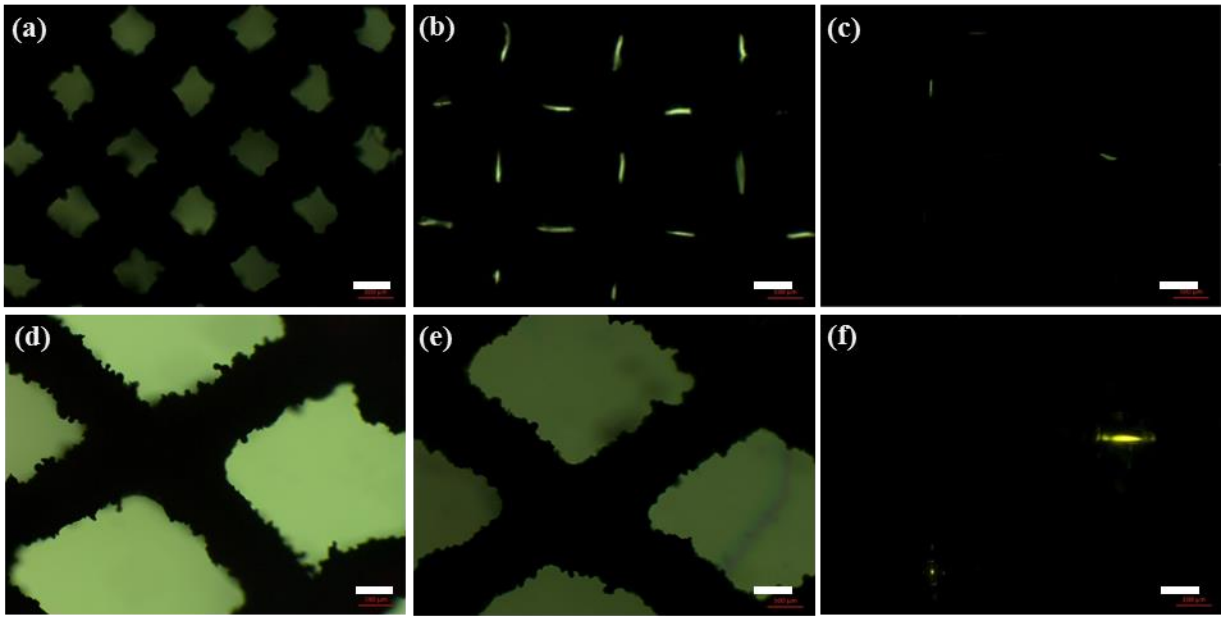

Figure 2. Transmitted light through 3D printed lattice structures. A lattice having a mesh size of 400 µm in the presence of (a) air, (b) water, and (c) crude oil. A lattice having a mesh size of 1000 µm under (d) air, (e) water, and (f) crude oil. Scale bars = 300 µm.

Figure 3 illustrates the light transmittance characteristics for a mesh size of 700 µm when different types of oil were presented. The shapes and colors of the light scattering out of the mesh dramatically changes for different types of oil. In Figure 3b and 3d, the transmitted light was highly intense for water and diesel, respectively, since these oil types are transparent liquids. In Figure 3c-e, the change in the wavelength of the transmitted light indicates the presence of oil. The presence of oil and other substances can be easily defined through the investigation of optical transmittance characteristics of these meshes. The transmitted light's spectrum and angular scattering is highly influenced by the properties of physical oils (refractive index, density and temperature).

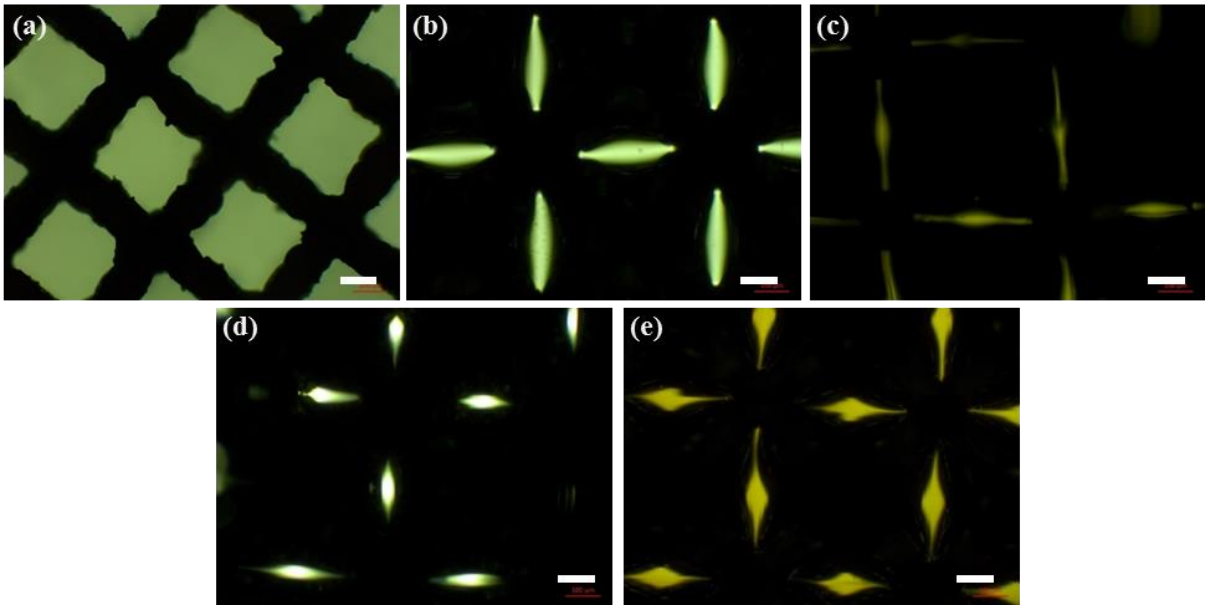

Figure 3. Transmittance optical images of lattice structures having a mesh size of 700 µm. Mesh in the presence of (a) air, (b) water and (c) crude oil, (d) diesel, (e) stroke oil. (Scale bars = 200 µm)

Light scattering experiments were conducted on the lattice microstructures in the presence of crude oil. Figure 4a-c shows the results of angle-resolved measurements of light transmission through the mesh using an automated rotational stage (Supporting Information Figure S2). Figure 4a shows the transmitted light (λ=532 nm) when the structure was empty. The light transmission (3.2 μW) was at normal incidence angle. When the mesh was submerged into the water, the transmitted light scattered through the mesh structure (Figure 4b). The intensity of the normally transmitted light decreased to 2.4 μW as the mesh was filled with oil (Figure 4c). The decrease was due to the angular scattering and also back reflection of light. In the presence of crude oil, the transmitted light decreased to ~0.1%. The light source and the detector were fixed at opposite sides of the mesh structures which were placed on the rotary stage. It was rotated 180° with increments of 1°. The 0° orientation was perpendicular to the face (Figure 1c-e). At 90°, the maximum transmission occurred for media, which were oil free. By adding water to the mesh structures, the transmission windows were narrowed which resulted in lower transmission intensity. The drastic decrease in light transmission in the presence of crude oil could be attributed to the high absorption property of most crude oil species (Figure 4f).

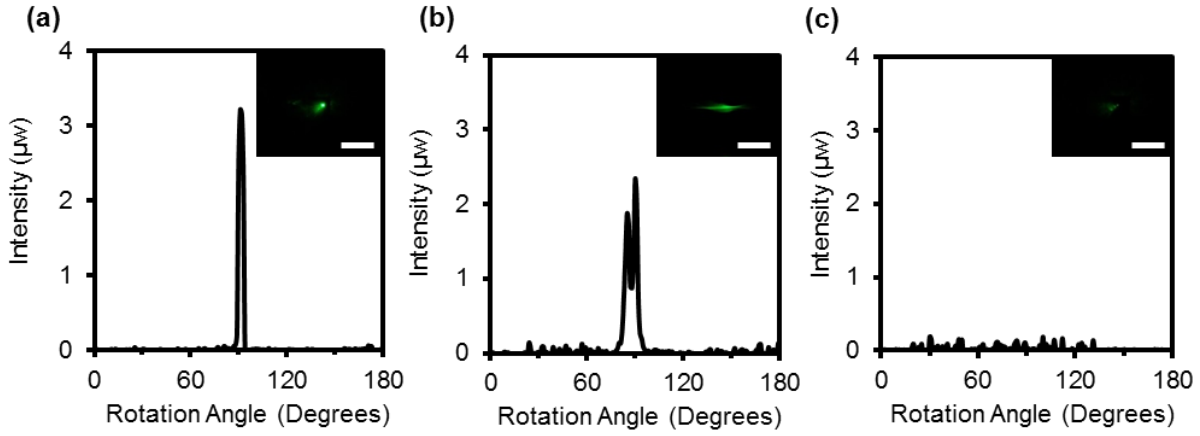

Figure 4. Transmitted light through the lattice structure having a mesh size of 700 μm. Angle-resolved measurements of the structure having (a) air, (b) water, and (c) crude oil. (Scale bars=1.5 cm).

Diesel and stroke oil were also tested to characterize light scattering behavior of the lattice structure. Angle-resolved measurements were carried out for the transmitted light corresponding to mesh structures having diesel and stroke oil. In the presence of diesel oil, the transmitted light pattern diffused and the intensity of the light was 1.2 µW, where the light was scattered from -15° to 20° from the normal (Figure 5a). When the light passed through the mesh in stroke oil, the transmitted light was focused with an intensity of 5.4 µW received at the central peak (Figure 5b). The study suggests that each oil species forms a different distribution and dimensions of droplets within the meshes, leading to distinct optical scattering and transmission properties. These distinctions can be used for oil detection and sensing by integrating these meshes with optic fiber detection.

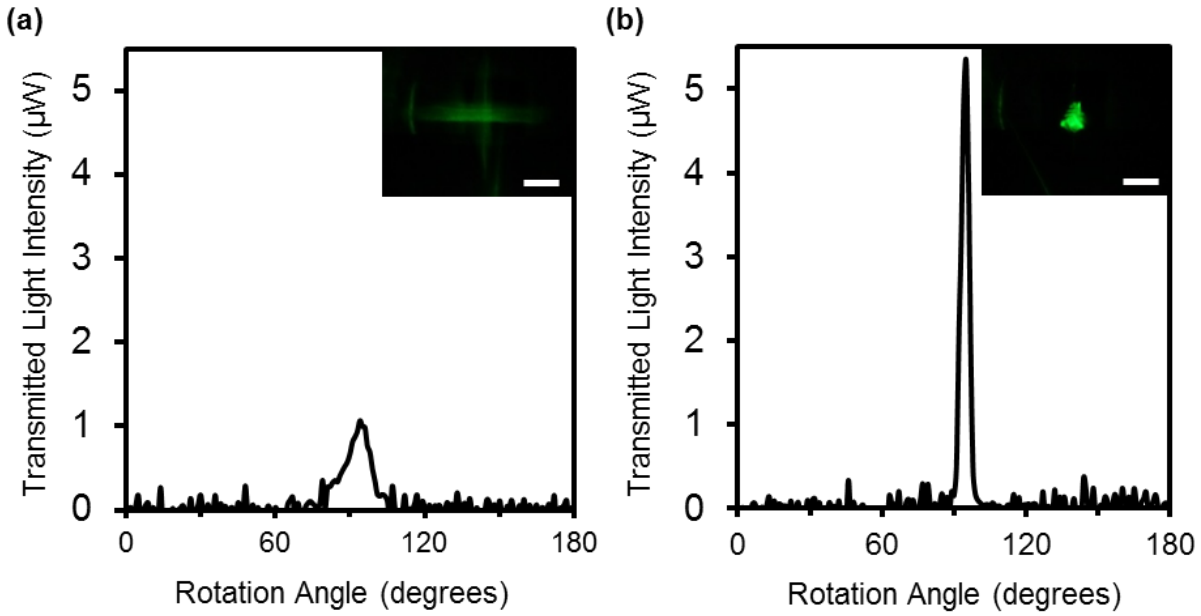

Figure 5. Transmitted light through the lattice structure having a mesh size of 700 µm. Angle-resolved measurements of the transmitted light from the structure soaked with (a) diesel, and (b) stroke oil. The insets show the photographs of the transmitted light. Scale bars= 2 cm.

The presence of different fluids in the mesh structure altered scattering characteristics of the transmitted light in terms of intensity and wavelength. To investigate the changes in the transmitted light wavelength, spectroscopy measurements were performed. The focusing behavior of the mesh structures (which produces discrete optical transmission windows) enabled the investigation of small field of view of the specimen in spectroscopy analysis, leading to significant reduction of stray light. Figure 6 shows transmitted light from the mesh in the presence of water, diesel, stroke oil, and crude oil. Figure 6a-b shows the transmittance of 400 μm and 1000 μm sized structures in the presence of crude oil as compared to water. Both meshes demonstrated analogous behavior. However, as the mesh size changed, the intensity of tranmittance was altered. Figure 6c demonstrates the spectrum of transmitted light through a mesh structure having a mesh size of 700 μm in the presence of different oils. Each oil type and water had different absorption values and demonstrated different optical transmission values from 400 to 800 nm. For the crude oil, the the global minimum for the transmitted light was at 500 nm and the local maximum was at 600 nm. Additionally, for the stroke oil, the spectrum was altered from the case when only water was present. By comparing the transmission spectra of the measured oils to the transmission spectrum of water, the spectra were found to be unique for each oil type. The intensity of the transmitted light spectrum might be varied depending on the measurement environment; however, the trends of the patterns remain analogous. Figure 6d shows that by considering the transmission spectrum obtained from oil measurements with respect to transmission from water, unique trends can be obtained. These measurements can be used as a fingerprint for each oil and provide a method for rapid detection of specific oil types. Once the measurements were performed, mesh structures were washed with water and dried out with nitrogen gas. To verify the complete removal of oil species, a spectroscopy measurement of cleaned mesh was performed which was consistent with initial spectroscopy measurements.

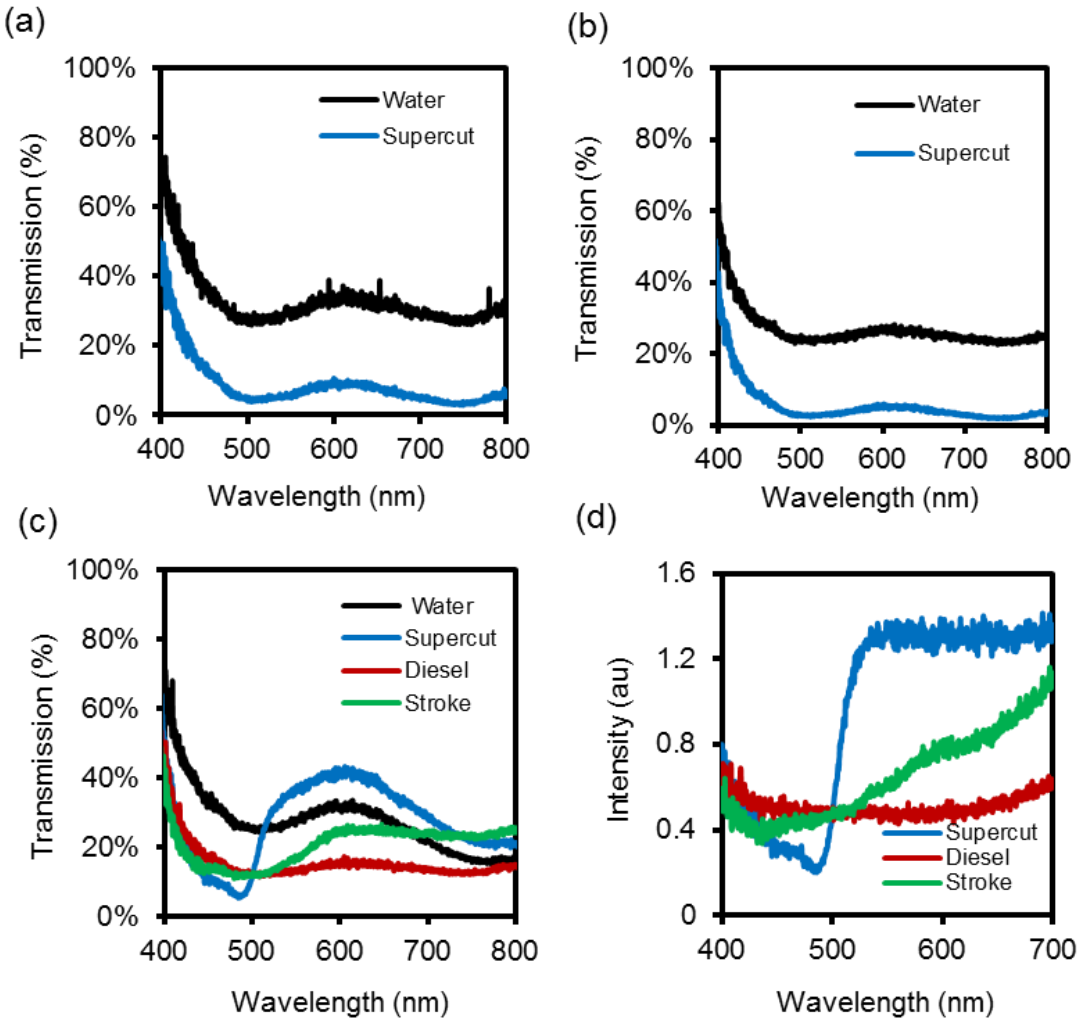

Figure 6. Spectroscopy measurements of the transmitted light through the mesh in the presence of different oil types. Crude oil measurements for (a) 400 µm, (b) 1000 µm, and (c) 700 µm, where empty mesh was used as reference. (d) Transmission spectrum for 700 µm considering the mesh with water as a reference.

Conclusion

We demonstrated a lattice structure as an oil sensor based on the light scattering and spectroscopy measurements. Different mesh sizes were analyzed for comparison of their optical characteristics. The results showed that the mesh structure could distinguish oil types by light scattering method or investigation of the tranmission spectrum. Once the oil was detected, the transmittance measurement was used for identifying the sub-oil species.

Trasmitted light from the mesh in the presence of three different oils were analyzed and each type of oil showed a unique transmission spectrum. We demonstrated a new oil detection method by using lattice mesh structure, which could be quick and low-cost method for identifying oil sub-types. Additionally, the same type of meshes have been used for repeat analyses with different types of oil, showing reusability. One of the limitations of the present technique is the requirement of bulky optical measurement setup. However, by the miniaturization of the measuring unit and embedding wireless transmission technologies, remote sensing of the oil contraminants in the environment can be achieved. Furthermore, the present sensing technology can be integrated with optical fibers [24-27], waveguides,[28] optical resonators,[29] and smartphone readers[30, 31] to obtain quantitative measurements based on plasmonic or wavelength shifts. We anticipate that the development of the three-dimensional microstructured lattices presented in this work will enable a new generation of sensing technology.

AUTHOR INFORMATION

Corresponding Authors

* h.butt@bham.ac.uk; k.e.a.essa@bham.ac.uk

Author Contributions

A.S. and R.S. performed the experiments and wrote the article. H.H. and K.E. fabricated the mesh structures. A.K.Y. and H.B. made intellectual contributions and edited the article.

Funding Sources

The authors thank Leverhulme Trust for research funding.

Notes

The authors declare no competing financial interests.

References

[1] A. K. Yetisen, Y. Montelongo, F. da Cruz Vasconcellos, J. L. Martinez-Hurtado, S. Neupane, H. Butt*, et al.*, "Reusable, Robust, and Accurate Laser-Generated Photonic Nanosensor," *Nano Letters,* vol. 14, pp. 3587-3593, 2014/06/11 2014.

[2] D. Gately, N. Al-Yousef, and H. M. Al-Sheikh, "The rapid growth of domestic oil consumption in Saudi Arabia and the opportunity cost of oil exports foregone," *Energy Pol.,* vol. 47, pp. 57-68, 2012.

[3] S. Yanxun, W. Yani, Q. Hui, and F. Yuan, "Analysis of the groundwater and soil pollution by oil leakage," *Procedia Environ Sci,* vol. 11, pp. 939-944, 2011.

[4] A. Agoston, C. Ötsch, and B. Jakoby, "Viscosity sensors for engine oil condition monitoring—Application and interpretation of results," *Sens. Actuator A-Phys.,* vol. 121, pp. 327-332, 2005.

[5] T. Wu, H. Wu, Y. Du, and Z. Peng, "Progress and trend of sensor technology for on-line oil monitoring," *Sci China Technol Sc,* vol. 56, pp. 2914-2926, 2013.

[6] E. Baszanowska and Z. Otremba, "Spectral signatures of fluorescence and light absorption to identify crude oils found in the marine environment," *J Eur Opt Soc Rapid,* vol. 9, 2014.

[7] L. Markova, N. Myshkin, H. Kong, and H. Han, "On-line acoustic viscometry in oil condition monitoring," *Tribol Int,* vol. 44, pp. 963-970, 2011.

[8] T. Takeo and H. Hattori, "Optical fiber sensor for measuring refractive index," *Japanese Journal of Applied Physics,* vol. 21, p. 1509, 1982.

[9] W. Jin, H. Ho, Y. Cao, J. Ju, and L. Qi, "Gas detection with micro-and nano-engineered optical fibers," *Optical Fiber Technology,* vol. 19, pp. 741-759, 2013.

[10] S. Deng, P. R. Kidambi, H. Butt, A. Sabouri, M. Sohail, S. A. Khan*, et al.*, "Optical scattering from graphene foam for oil imaging/sensing," *RSC Advances,* vol. 6, pp. 71867-71874, 2016.

[11] C. Chu, G. Graf, and D. W. Rosen, "Design for additive manufacturing of cellular structures," *Computer-Aided Design and Applications,* vol. 5, pp. 686-696, 2008.

[12] L. J. Gibson and M. F. Ashby, *Cellular solids: structure and properties*: Cambridge university press, 1999.

[13] S. Yoshida, K. Suizu, E. Kato, Y. Nakagomi, Y. Ogawa, and K. Kawase, "A high-sensitivity terahertz sensing method using a metallic mesh with unique transmission properties," *Journal of Molecular Spectroscopy,* vol. 256, pp. 146-151, 2009.

[14] Y. Han, J. Lin, Y. Liu, H. Fu, Y. Ma, P. Jin*, et al.*, "Crackle template based metallic mesh with highly homogeneous light transmission for high-performance transparent EMI shielding," *Scientific reports,* vol. 6, 2016.

[15] T. Kondo, S. Kamba, K. Takigawa, T. Suzuki, Y. Ogawa, and N. Kondo, "Highly sensitive metal mesh sensors," *Procedia Engineering,* vol. 25, pp. 916-919, 2011.

[16] M. Ashby, "The properties of foams and lattices," *Phil. Trans. R. Soc. A,* vol. 364, pp. 15-30, 2006.

[17] L. E. Murr, S. M. Gaytan, E. Martinez, F. Medina, and R. B. Wicker, "Next generation orthopaedic implants by additive manufacturing using electron beam melting," *Int J Biomater,* vol. 2012, pp. 1-14, 2012.

[18] D. Gu, W. Meiners, K. Wissenbach, and R. Poprawe, "Laser additive manufacturing of metallic components: materials, processes and mechanisms," *Int Mater Rev,* vol. 57, pp. 133-164, 2012.

[19] L. Hao, S. Dadbakhsh, O. Seaman, and M. Felstead, "Selective laser melting of a stainless steel and hydroxyapatite composite for load-bearing implant development," *J Mater Process Tech,* vol. 209, pp. 5793-5801, 2009.

[20] Y. Li, Y. Tian, C. Yang, D. Zhang, and X. Liu, "Laser-induced hydrophobicity on Ti-6Al-4V surface," in *2015 International Conference on Manipulation, Manufacturing and Measurement on the Nanoscale (3M-NANO)*, 2015, pp. 153-158.

[21] K. M. Knowles, H. Butt, A. Batal, A. Sabouri, and C. J. Anthony, "Light scattering and optical diffusion from willemite spherulites," *Optical Materials,* vol. 52, pp. 163-172, 2// 2016.

[22] H. Butt, K. M. Knowles, Y. Montelongo, G. A. J. Amaratunga, and T. D. Wilkinson, "Devitrite-Based Optical Diffusers," *ACS Nano,* vol. 8, pp. 2929-2935, 2014/03/25 2014.

[23] Q. Dai, R. Rajasekharan, H. Butt, X. Qiu, G. Amaragtunga, and T. D. Wilkinson, "Ultrasmall microlens array based on vertically aligned carbon nanofibers," *Small,* vol. 8, pp. 2501-2504, 2012.

[24] J. Guo, X. Liu, N. Jiang, A. K. Yetisen, H. Yuk, C. Yang*, et al.*, "Highly Stretchable, Strain Sensing Hydrogel Optical Fibers," *Adv Mater,* vol. 28, pp. 10244-10249, Dec 2016.

[25] A. K. Yetisen, N. Jiang, A. Fallahi, Y. Montelongo, G. U. Ruiz-Esparza, A. Tamayol*, et al.*, "Glucose-Sensitive Hydrogel Optical Fibers Functionalized with Phenylboronic Acid," *Advanced Materials. DOI: 10.1002/adma.201606380,* 2017.

[26] M. Humar, S. J. Kwok, M. Choi, A. K. Yetisen, S. Cho, and S.-H. Yun, "Toward biomaterial-based implantable photonic devices," *Nanophotonics,* vol. 1, pp. 0-11, 2016.

[27] A. A. Rifat, R. Ahmed, A. K. Yetisen, H. Butt, A. Sabouri, G. A. Mahdiraji*, et al.*, "Photonic Crystal Fiber Based Plasmonic Sensors," *Sensors and Actuators B: Chemical,* 2016.

[28] R. Ahmed, A. A. Rifat, A. K. Yetisen, S. H. Yun, S. Khan, and H. Butt, "Mode-multiplexed waveguide sensor," *Journal of Electromagnetic Waves and Applications,* vol. 30, pp. 444-455, 2016.

[29] R. Ahmed, A. A. Rifat, A. K. Yetisen, M. S. Salem, S.-H. Yun, and H. Butt, "Optical microring resonator based corrosion sensing," *RSC Advances,* vol. 6, pp. 56127-56133, 2016.

[30] A. K. Yetisen, J. Martinez-Hurtado, A. Garcia-Melendrez, F. da Cruz Vasconcellos, and C. R. Lowe, "A smartphone algorithm with inter-phone repeatability for the analysis of colorimetric tests," *Sensors and Actuators B: Chemical,* vol. 196, pp. 156-160, 2014.

[31] J. L. Martinez-Hurtado, A. K. Yetisen, and S.-H. Yun, "Multiplex Smartphone Diagnostics," *Multiplex Biomarker Techniques: Methods and Applications,* pp. 295-302, 2017.